State Machine-Based Architecture to Control System Processes in a Hybrid Fuel Cell Electric Vehicle

Ali Molavi[a,*], Attila Husar[a], Hampus Hjortberg[b], Niclas Nilsson[b], Markus Kogler[c], Juan Sanchez Monreal[d], Yousif Eldigair[e,a], Maria Serra Prat[a]

[a]*Institut de Robotica i Informatica Industrial, CSIC-UPC, Barcelona, Spain*
[b]*PowerCell, Gothenburg, Sweden*
[c]*AVL, Graz, Austria*
[d]*German Aerospace Center (DLR), Institute of Engineering Thermodynamics, Pfaffenwaldring 38-40, 70569, Stuttgart,, Germany*
[e]*Brose Fahrzeugteile SE CO., Würzbrug, Germany*

Abstract

In this paper, a fuel cell system supervisory controller is developed and implemented in a hydrogen-based fuel cell electric vehicle to safely control the fuel cell system processes and coordinate the communication between the balance of plant subsystems, vehicle control unit, diagnosis unit and, powertrain part. The developed supervisory controller includes three main parts: State Machine, Optimal Setpoint Generator, and Power Limit Calculator. The state machine as the central part of the supervisory controller, coordinates the different operation states of the fuel cell system, including the complex processes of start-up and shutdown. To maximize the fuel cell system efficiency and minimize the degradation of the stack an optimal setpoint generator that produces the subsystem's setpoints is implemented by solving an optimization problem and considering the manufacturer's requirements. The power limit calculator is dedicated to estimate the power that can be delivered by the stack. Furthermore, it calculates the DC/DC current setpoint and delivers this information to the Energy Management System (EMS) that manages the requested power between the battery and the fuel cell system. The Worldwide harmonized Light vehicles Test Cycles (WLTC) are used to verify the functioning of the proposed fuel cell system supervisory controller

*Corresponding Author
Email address: ali.molavi@upc.edu (Ali Molavi)

in a real car. The designed control structure is implemented in a prototype hydrogen-based electric car at both PowerCell and CEVT facilities under the framework of INN-BALANCE Horizon 2020 European project.

Keywords: Supervisory controller, PEM fuel cell, Hydrogen based electric vehicle, State Machine, Optimal setpoint generator

---

1. Introduction

Fuel cell electric vehicles have been increasingly under development due to their ability to provide extended driving ranges at zero-emission[1]. However, this type of vehicle faces several challenges. The lifetime and durability of a fuel cell system is a key point in developing fuel cell vehicles and, it is a critical factor for end-user acceptance[2]. Among the different types of Fuel Cells (FCs), Polymer Electrolyte Membrane fuel cells (PEMFC) are the most extensively researched technology all over the world due to their suitability for automotive and portable applications[3]. In automotive applications, the fuel cell systems have to be able to adapt to a wide range of operating conditions given by start-up and shutdown processes, sudden load changes or varying power levels[4]. The durability and lifetime of the stack are affected by the operating conditions (temperature, humidity, pressure, mass flow rate, etc.) during drive cycles, idling, start-up and shutdown procedures, and other states of the power system. The load cycle in automotive applications causes the cyclic change in the stoichiometric ratio and pressure of the supplied gases, which makes the gas starvation very possible. In addition, the electrochemically generated water and heat inside the fuel cell vary with changes in load. Eventually, this creates an internal environment of thermal/humidity cycling that radically accelerates catalyst aging and mechanical degradation of components[5]. Therefore, operating in the optimal operation condition is very important to diminish these effects. In terms of operating conditions, researchers have published many works focused on the optimization of operating conditions for the automotive applications. In [4], a quasi-steady fuel cell model of the fuel cell system integrated into the vehicle model was developed and is used to optimize the air pressure and mass flow rate to maximize system efficiency. Another strategy is proposed in [6] to maximize the system performance. However, the pressure is assumed to be constant and the loss consumption is not considered. A model reference adaptive control was presented in [7] to maximize the efficiency considering

the optimal oxygen ratio. However, the temperature and humidity ratio are assumed to be constant and there is no experimental implementation. In [8], the optimal operating temperature corresponding to the point with the fuel cell's largest efficiency is obtained through a fuel cell based truck test bench and a model predictive control was proposed to control the temperature. The Particle Swarm Optimization (PSO) algorithm was proposed in [9] to optimize the operating conditions and design parameters of a high-temperature PEMFC-based vehicle. However, the algorithm is not applicable in real vehicle due to its high computation time and the optimal conditions for different load of current were not reported.

In addition to the dynamic change of load and the need to work in optimal operating conditions, the working state of the automotive fuel cell imposes other states, such as start-up and shutdown that cause degradation and decrease in the useful life of the PEMFC. The start-stop state contributes about 33%to the degradation of PEMFC during operation [10]. Therefore, the application of strategies to mitigate the degradation of the stack is required for PEMFC systems, especially for transportation systems undergoing thousands of start-up and shutdown events during their lifetimes. One of the challenges in the start-up and shutdown procedure is freeze start-up and shutdown. Starting a fuel cell at a sub-freezing temperature always has been a challenge due to the freezing the produced water. Due to the ice formation inside the stack, the cathode channel is blocked and the stack is not able to produce power and the start-up failed. A successful cold start requires the cell to raise the temperature above the freezing point before the cathode catalyst layer is blocked with ice [11]. Cold start strategies can be divided into the self-cold start and assisted cold start according to the heating sources. Self-cold start completely relies on the heat released by the electrochemical reaction, which is usually achieved by controlling the load, i.e., galvanostatic mode[12]. However, due to low water content during the start-up, the stack cannot support high current density and the self-heating capability of the stack is not enough. So, potentiostatic mode was proposed by work [13]. Ramping the current was proposed by [14] and control of the output power was proposed by [15] despite this strategy is adequate at relatively high temperatures. The assisted cold start-up in which extra heat is applied to do the cold start-up, can compensate the lacks of the self-cold start-up. Montaner Ríos et al. in[16] proposed a coolant heating strategy to heat a 4kW PEMFC. They used the cooling subsystem to heat the stack

during the start-up. To have a successful start-up and shutdown, removing the generated water is important. In [17], an effective gas purge as a key step to remove the residual water inside the cell and subsequently prevent the ice formation in the cathode catalyst layer was proposed. Apart from the start-up and shutdown issues, in some conditions of PEMFC vehicles, such as climbing or acceleration, the fuel cell operates under high power conditions for short durations. Meanwhile, owing to the effect of compressor dynamic and gas inertia, there would be serious gas starvation which is harmful to the fuel cell stack[18]. In this work, a strategy is proposed where the actual current of the fuel cell equal to the DC/DC converter current setpoint is calculated based on the available amount flow of air that enters at the inlet of the stack, therefore, the probability of gas starvation decreases. As aforementioned in[4, 5, 6, 7, 8, 9] and [11, 12, 13, 14, 15, 16], most of the existing experimental researches mainly focus on laboratory scale fuel cells and there are not enough reports that involve PEMFC application in a real vehicle. Especially, there are not many studies that proposed a thorough fuel cell system control unit that covers all the necessary parts to improve the fuel cell durability and system reliability in an automotive application. In addition, the capacity to be implemented in a real vehicle is essential. The main objective of this paper is to design and implement a fuel cell system supervisory controller (FCSSC) based on a state machine architecture for a Fuel Cell Electric Vehicle (FCEV). The considered Fuel Cell System (FCS) is a complex system with multiple states of operation. This includes the Start-up, Run, Shut-down and Idle states, which have been identified as the states of a State Machine (SM). Furthermore, the FCS incorporates several subsystems, namely, the cathode, the anode, the thermal subsystems and the DC/DC converter that all have different modes of operation. In each specific state of the FCS, the subsystems operate in different modes of operation. Therefore, a control structure is necessary to coordinate these subsystems and the stack in the different FCS operation states and the operation modes of the different subsystems. The main contributions and parts of this work are summarized as follows:

- Design a FCSSC using a State machine to control all the fuel cell system processes in an automotive application
- Design an offline optimal setpoint generator that computes the subsystems setpoints that maximize the efficiency and takes into consideration

all the manufacturer limitations to minimize degradation in the Run state.

- Minimizing the damage of the stack, especially in the high power demanded conditions such as climbing and acceleration. This is done by estimating the immediate and future fuel cell stack power capabilities. This estimation is based on the stack variables measurements and it is fed to the vehicle's energy management system (EMS). Furthermore, the DC/DC current setpoint is calculated based on the available air mass flow at the inlet of the stack to prevent air starvation or high-power extraction.

- Propose a start-up strategy that combines the advantages of self-cold start using the ability to operate in potentiostaic or galvanostatic mode and coolant heating assisted cold start. Furthermore, compressor air blowing is used in the start-up and shutdown to remove the generated water and help to prevent ice formation

- As the purpose of INN-BALANCE project, develop advanced balance-of-plant components (BoP) for current generation of fuel cell-based vehicles, the designed FCSSC was implemented in the real prototype vehicle in PowerCell and CEVT facilities. The INN-BALANCE consortium was composed industrial actors (BRO, AVL, CEVT, AYE), research and technology organizations (DLR, S2i), SMEs with research capabilities (CEL, PCS) and a higher research institution (UPC).

2. Fuel cell system description

2.1. Fuel cell stack and the balance of plant subsystems description

The fuel cell system implemented in this work is shown in Fig.1. It includes four auxiliary subsystems, i.e., anode, cathode, thermal, and power electronic subsystems, apart from the PEMFC stack. The hydrogen is stored in a pressurized tank and is delivered to the stack anode channel through the anode subsystem. The unused hydrogen, which exits in the stack has to be recovered and recirculated to increase the hydrogen utilization rate and overall efficiency of the FC system. An ejector-injector in the recirculation path is used to increase the utilization rate of hydrogen and to maintain a more uniform concentration in the stack. The anode subsystem is equipped with a water separator and a purge valve to remove the accumulated liquid

water and, the nitrogen diffused through the membrane from the cathode to the anode side. A hydrogen heat exchanger for pre-heating is incorporated in the anode module in order to avoid condensation when cold dry hydrogen is mixed with warm humid nitrogen and hydrogen coming out from the stack outlet. Partner AVL[1] developed the anode subsystem. The cathode subsystem is in charge of delivering the demanded air flow to run the fuel cell. It is equipped with a turbo-compressor with air-bearings, which, compared to conventional oil-bearings, guarantees that the air supply remains pure and uncontaminated. Furthermore, by using gas-bearings, frictional losses are reduced and the lifetime of the compressor is extended. To ensure the proper functioning of the fuel cell stack, the pressure, mass flow, temperature and humidity of the air to be fed into the stack are constantly monitored and controlled. Partner BROSE[2] coordinated the development of the cathode subsystem. The operating stack temperature has to be kept in the proper range to maintain optimum electrochemical reactions and keep the integrity of the PEMFC stack material. The thermal subsystem provides a coolant flow to remove the generated heat through a radiator. In addition, the thermal subsystem is equipped with a heating circuit including a pump and a heater to heats the stack in the subfreezing start-up. Partner DLR [3] developed the design and concept of the thermal management system. Finally, the power electronic subsystem is in charge of the electric power conditioning and is developed by the CEVT[4].

[1]AVL List GmbH, Engineering Service Provider

[2]Brose Mechatronics, Germany

[3]German Aerospace Center (DLR), Institute of Engineering Thermodynamics, Stuttgart, Germany

[4]China Euro vehicle technology

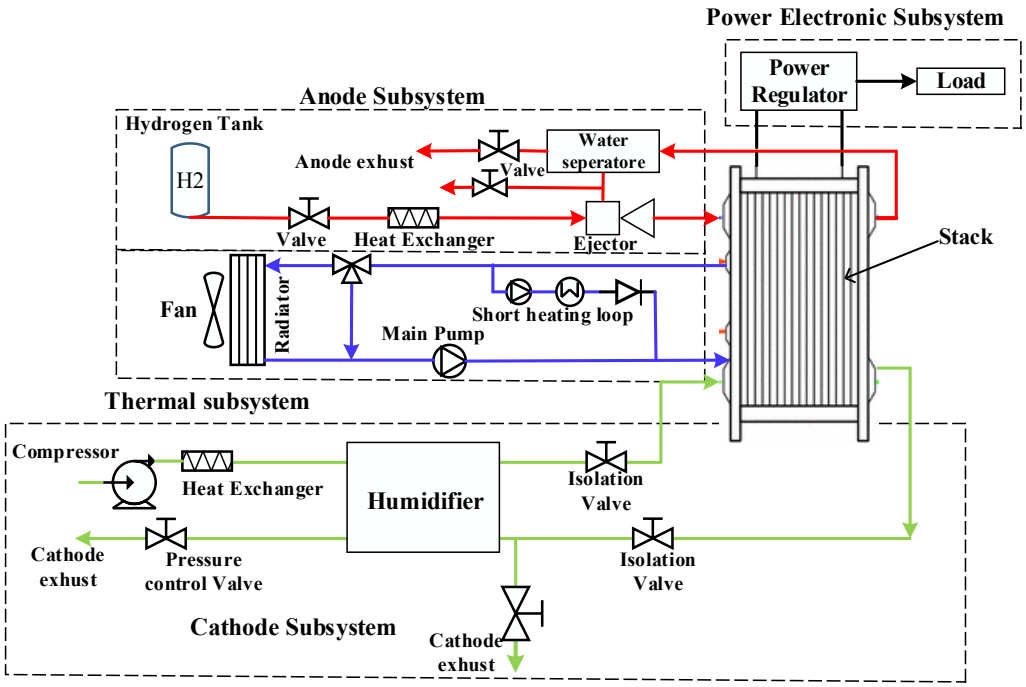

Figure 1: Fuel cell stack and the auxiliary subsystems

3. Supervisory Controller design

In this section, a novel FCSSC is proposed and described. Supervisory controllers distribute the system's global requests to particular requests necessary from individual subsystems or components of the system equipment set. The individual demands are translated into the setpoints of the local controllers[19]. The proposed fuel cell supervisory controller integrated with the individual control elements of the vehicle propulsion system is shown in Fig.2. As it can be seen, the fuel cell hybrid electric vehicle's overall control system architecture is divided into different layers. The highest level of control is the Vehicle Control Unit. The second level, which is the focus of this work, is the FCSSC. It comprises three main parts; State Machine (SM), Optimal Setpoint Generator (OPSG), and Power Limit Calculator (PLC). The FCSSC developed in this work is a hybrid control system that includes a discrete event control system which decides when to activate the distinct operating states and sub-states, and it includes a control system in charge of the continuous generation of proper setpoints for the subsystem's local

controllers. The discrete event controller of this work is a state machine developed with Stateflow and the continuous control system is implemented as an optimal setpoint generator linked to the local controllers. Furthermore, the supervisory controller includes an algorithm to estimate the available stack power which is the Power Limit Calculator. The supervisory controller receives all the information from the input wrapper, which collects 33 input signals. These include commands from the Vehicle Control Unit (VCU), estimation results from the observer, and diagnostic results from the diagnostic unit. The supervisory controller uses the collected information to automatically coordinate the subsystems, determines local controller setpoints, determines DC/DC converter current setpoint and estimates stack available power information for the VCU. The diagnosis unit is in charge of diagnosing hardware failure such as sensors failure, compressor errors, etc. The third level includes the ancillary subsystem's local controllers, i.e., anode, cathode, and thermal subsystem's controllers. Each subsystem controller (SSC) is programmed with local control algorithms to achieve the setpoints received from the FCSSC at the upper level.

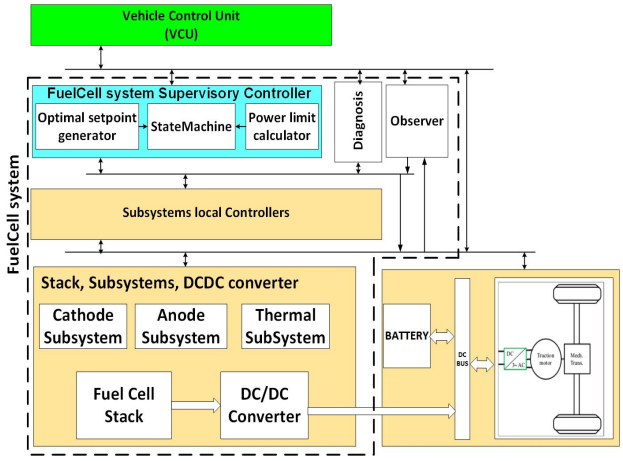

Figure 2: Control Layered structure in this work

3.1. Functionality of State machine

A complex system as a vehicle has different states of operation, corresponding to different functions. The operation states of the fuel cell system in this automotive application are: Initial, Failsafe, Standby, Refueling, Service mode, Start-up, Run, Min Power, Normal shutdown and Fast shutdown.

The overall scheme of the proposed SM is shown in Fig.3. In each operation state, the SM manages the activation of the different modes of operation of the different subsystems. The output of the SM are the protocol numbers, the setpoints for the subsystems and the error detection flags implemented inside SM.

3.1.1. Protocol numbers and status numbers

The SM uses protocol numbers and status numbers to communicate with the subsystems. There are four protocol/status numbers, for the cathode, thermal, anode and DC/DC subsystems, respectively. The numerical values of each of the protocol/status number refer to specific modes of operation of the different subsystem, as seen in Table 1. The protocol number and the status number use the same numerical values. The different operation modes of the four subsystems and the assigned protocol numbers to their different operation modes are listed in Table 1. The supervisory controller commands to change the mode of the different subsystems by sending to them the corresponding protocol number. After receiving the command, the subsystems respond by changing their operation mode and, subsequently, return the updated status number to the SM. An example is explained in section 3.1.3.

Table 1: Subsystem operation's modes and their corresponding protocol numbers and status numbers

Cathode Operation Modes	Protocol and Status number	Thermal Operation Modes	Protocol and Status number	Anode Operation Modes	Protocol and Status number	DC/DC Operation Modes	Protocol and Status number
Off	0	Off	0	Off	0	Standby	0
Bypass Humidification	1	Heating loop without heater	1	Start-up	1	Galvanostatic	1
Start Compressor Bypass air	2	Heating loop with heater	2	Run	2	Potentiostatic	2
Min flow	3	Cooling loop	3	Shutdown	3	Passive	5
Run	4	Cooling Loop for isolation	4			Error	15
Max flow	5						

3.1.2. SM cycle

The overall scheme of the SM is shown in Fig.3. In each state or substate of the SM, this state or substate is in charge of determining all the SM outputs. The fuel cell supervisory control unit is turned on when the vehicle is started and the onboard computer turns on. The SM starts in the initial state named 'Initialization'. At this point, all subsystems remain inactive. If the different subsystems report their successful initialization, the SM moves to the 'Standby' state and waits until the 'Run-Requested' is activated by the VCU. In the 'Standby' state, all the subsystems are still off except the

thermal subsystem where the main pump is turned on to clean up any ions in the coolant liquid inside the stack by the circulation of the coolant liquid in the thermal loop. Once the 'Run-Requested' is activated, the SM moves to the next state where the 'Start-up' procedure starts. In the 'Start-up' state the various subsystems are activated based on the defined procedure. The 'Run' state is activated after the startup procedure is completed and if the 'Run_Requested' is still active. When necessary, the driver stops the vehicle and the fuel cell system moves to 'Min Power' state. From this state, the system can come back to the 'Run' state again in the case of red light or move to the 'Normal Shutdown' as shown in Fig.3. If the system's state changes to 'Normal Shutdown', the subsystems have to be turned off in an orchestrated manner by receiving ordered protocol numbers to avoid damage to the fuel cell stack. After the Shutdown is finished, the fuel cell system moves to 'Standby' state. In the case of a malfunction in one of the subsystems or components, the 'Failsafe' state is triggered and the whole system is depowered. The 'Failsafe' state has the highest priority among the other states of operation. In the next section, the Start-up and Shutdown procedures are explained

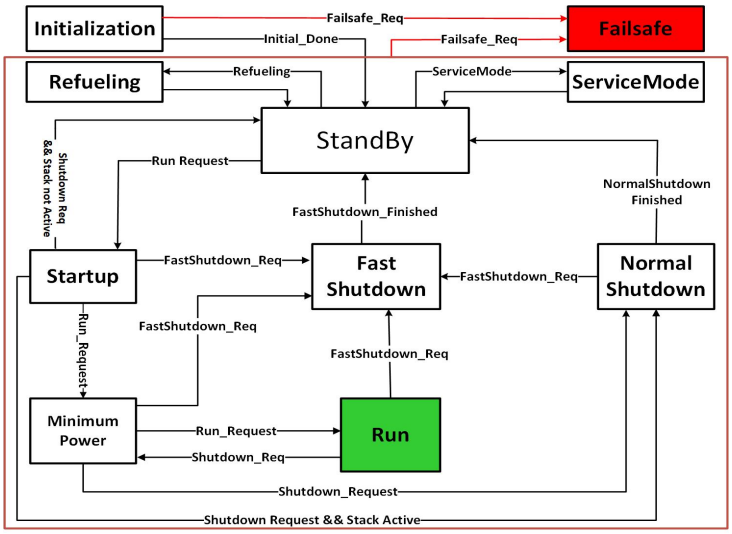

Figure 3: Overall scheme of the SM

3.1.3. Start-up procedure

During the 'Start-up' procedure, the SM sends the protocol numbers and setpoints to the subsystem controllers to start the different subsystems. The SM gets feedback from the subsystems with the sensors and the status variables. The start-up procedure is shown in Fig.4(a).The start-up shows how the different modes of operation of the subsystems are activated when the SM travels along the different substates inside the start-up state. The condition to transit from one substate for example, 'start compressor bypass' to the next substates, 'cathode min flow' and 'anode start-up', is to receive a status number from the cathode subsystem that verifies the compressor started successfully; otherwise, the SM remains in the previous substate until a timeout is reached and the 'Failsafe' is activated. The status numbers are shown with $SN\_X = k$. The indexes k and X are the corresponding status number for the subsystems which are listed in Table1. $SN\_Ca = 2$ means that the cathode subsystem has returned successfully the status number corresponding to the protocol number 2. Fig.5(a) shows the activation signals for the first 40 seconds of a 'Normal Start-up' in the real vehicle. It shows the change in the protocol number of the different subsystems to do a successful start-up. It also shows two of the locally controlled measurement variables: the mass flow of air and inlet coolant temperature. The mass flow of the compressor increases when the protocol number of the cathode changes from 0, then decreases to a setpoint value for protocol number = 4 at $t = 14$ s. In this test, the stack temperature is $T\_stack > 33°C$ and the 'heating loop without heater' is activated in the thermal subsystem with protocol number= 1 and then at $t = 14$ s, the 'cooling loop' is activated and the temperature of the coolant decreases due to the volume of water inside the radiator. After $t = 23$ s, the temperature increases due to electrochemical reaction inside the stack to reach a defined temperature setpoint. The setpoints of these variables are defined by the SM. In the case of low temperature, the proposed strategy in this work is to use the thermal subsystem which applies extra heat to do the assisted cold start-up. This action is done in the second step of the start-up procedure by activating the 'Thermal heating circuit with heater'. To remove the generated water and prevent ice formation, the cathode subsystem feeds the stack with the maximum flow by activating the mode 'Cathode Max flow (Dry stack)'. Results of the tests in the real prototype vehicle showed that the proposed SM structure can successfully perform the start-up process for an automotive application.

3.1.4. Shutdown procedure

During the Shutdown procedure, the same SM communication strategy is followed as for the start-up procedure. The state machine sends the protocol numbers and setpoints to the subsystem controllers to shut down the different subsystems. The shutdown procedure is shown in Fig.4(b). It shows how the different modes of operation of the subsystems are activated through the protocol numbers. The condition to transit from one substate such as 'Cathode Max flow' to the next substate, 'Cathode min flow' is indicated on the arrows from the initial state to the final state. If these conditions do not achieve, the SM will remain in the previous substate until a timeout is reached and the 'Failsafe' is activated. Fig.5 shows the activation signals for $t > 540$ s of a normal shutdown and how all the subsystems are shut down based on the programmed shutdown procedure. It also shows two of the measurements of the locally controlled variables: the cathode inlet mass flow of air and the inlet coolant temperature. The mass flow of the compressor decreases when the protocol number of cathode changes from 4 to 1, then increases to a maximum value of $50(g/s)$ for protocol number = 5 at $t = 550$ s to dry the stack. In this test, the stack temperature is $T\_stack \approx 69°C$ and the 'Cooling loop' is activated in the thermal subsystem with protocol number 3 and then at $t = 546$ s, the setpoint of the inlet coolant is set to $60°C$ as the shutdown temperature to cools down the stack. The inlet coolant temperature and as a consequence the outlet coolant temperature decreases to reach a safe shutdown temperature. The experimental results in Fig.5 have shown that in the real prototype vehicle, the proposed SM framework can successfully perform the fuel cell system processes and the fuel cell system has a successful start-up and shutdown.

3.1.5. Run state

During the 'Run' state, the demanded power by the vehicle is converted to the corresponding current and the setpoints are generated based on this demanded current. Furthermore, the Power Limit Calculator computes the DC/DC current setpoint and the stack available power information based on the measurement signals. The SM receives setpoints of the BoP subsystems from the optimal setpoint generator and the DC/DC current setpoint from Power Limit Calculator and sends these setpoints to the different subsystems and DC/DC converter More details will be found in section 4. In the following, two other parts of the supervisory controller will be described and their role in the FCSSU will be explained.

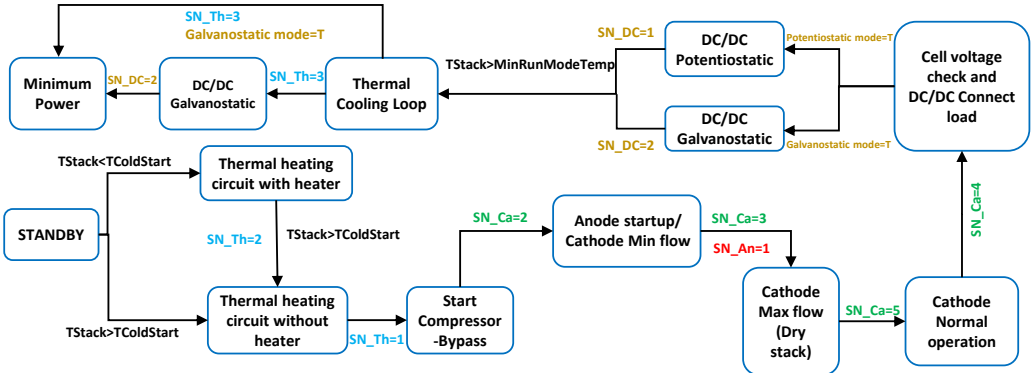

(a)

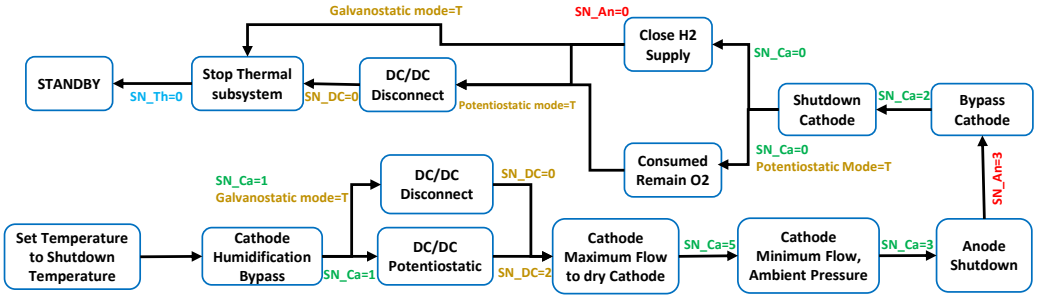

(b)

Figure 4: (a)Start-up procedure sub-state machine.(b) Shutdown procedure sub-state machine

3.2. Optimal setpoint generator

Considering the issues that arise as a result of operating in an adverse operating point, it is important to find the optimal operating condition for each load power and keep the fuel cell system working in that condition. The operation conditions include inlet air pressure, mass flow rate and humidity ratio, hydrogen pressure,and stack temperature. These operating conditions are in fact, the setpoints for the different subsystems and are tracked by each of the SSCs. The optimal setpoint generator is a part inside the supervisory controller that is executed during the 'Run' state and generates these optimal operation conditions. The generated setpoints are delivered to the state machine as shown in Fig.7. It is important to note that during other states of operation such as the 'Startup' and 'Shutdown', the subsystem local controller setpoints are defined inside the State machine based on the practical

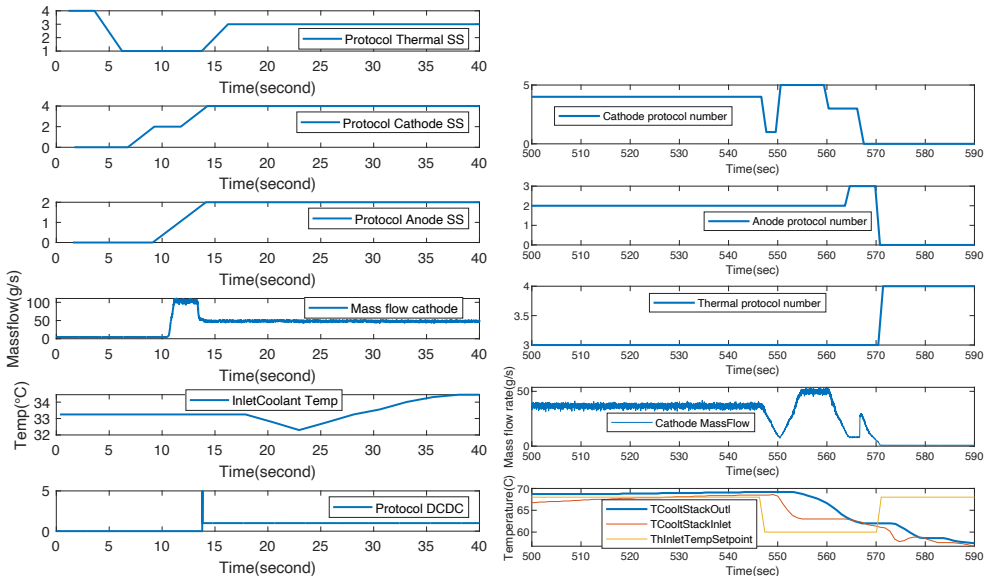

(a) Activation of subsystems in the Start-up procedure

(b) Activation of subsystems in the Shutdown procedure

Figure 5: Measured activation signal of the subsystems in Startup and Shutdown procedure

and manufacturing requirements. The State machine as the central part of the fuel cell supervisory controller feeds these setpoints to the subsystem local controllers during the different states of operations. As the computation burden is very important in the implementation of an algorithm or controller in the automotive application, in this project an offline optimal setpoint generator, which is an offline map was proposed and implemented. MPC could achieve online optimized solutions, however, the real-time operation of the MPC presented in the literature is still not possible due to the high computation time[20]. The optimal setpoint generator finds the optimal setpoints corresponding to each load power, to maximize the fuel cell system efficiency. The requested load power is converted to the corresponding current first and then the current is the input of the optimal setpoint generator, that gives the corresponding optimal setpoints. More details about the optimal setpoint generator can be found in the previous work[21]. PEMFC efficiency, which is defined as the ratio of the net generated power to the enthalpy of reaction of the fed hydrogen, is computed as follows:

$$\eta = \frac{P_{net}}{HHV \cdot \dot{n}_{H_2}} = \frac{IV_{fc} - \sum_{s=subsystems} P_s}{HHV \cdot \dot{n}_{H_2}} \tag{1}$$

where $\dot{n}_{H_2}$ is the fuel out of the H_2 tank, and the HHV the higher heating value of hydrogen. IV_{fc} is the gross electrical power generated by the fuel cell and P_s is the electrical power consumed by the subsystems. The optimal setpoints corresponding to the load current are shown in Table3.

Table 2: Optimal setpoints based on the stack current

Current	$r_1 = \dot{m}_{cathode}$	$r_2 = p_{cathode}$	$r_3 = h_r$	$r_4 = p_{anode}$	$r_5 = T_{in}$	$r_6 = \Delta T_{thermal}$
60	25.68	1.18	0.12	0.2	68	2
100	28.15	1.28	0.12	0.2	68	2
150	34.49	1.39	0.12	0.2	68	4
200	48.098	1.61	0.12	0.2	68	8
250	56.047	1.63	0.12	0.2	68	10
300	66.82	1.75	0.12	0.2	68	12
350	75.91	1.95	0.095	0.2	68	12
400	86.45	1.97	0.095	0.2	68	12
450	94.83	2.08	0.07	0.2	68	12

3.3. Power limit calculator

One of the functionalities of FCSSC is to computes the available range of power that the fuel cell stack can deliver and sends this information to the vehicle control unit's energy management system. The energy management system uses this information to manage the power requested by the traction components, between the fuel cell stack system and the battery. The information that the FCSSC delivers to the energy management system are as follows: Maximum power, Maximum power ramp-up rate, Maximum instant power, and DC-DC set-point current. Using this information, the power requested to fuel cell system does not exceed the capability of the system, which is very important to minimize stack degradation and/or damage. In the following sections, more details about each output calculation are presented.

3.3.1. Maximum power

The maximum power is the maximum net power the fuel cell is expected to be able to deliver if given enough time to change the fluid dynamic state, based on the current stack temperature and membrane hydration conditions. The maximum power is the value that will limit the power supplied by the fuel cell system. Due to the slow dynamics of the stack temperature and the hydration conditions compared with the dynamics of the air compressor, the time constants of stack temperature and hydration condition are larger than the time constants of inlet air pressure and mass flow rate, which

are smaller than 3 s. The only parameters that affect the maximum power are the stack temperature and the hydration conditions, represented by the Electrochemically Active Surface Area (ECSA). The ECSA is a measure of the total active Pt available in the carbon-support layer at the cathode CL (CCL), and it depends on the Pt loading of the CCL, the pore distribution, the degradation condition of the stack, and the CCL hydration state[22]. As the CCL hydration state changes in dynamic load profile such as automotive application. So, the ECSA could be and is chosen as an effective index to show the hydration state of the stack. In this work using the experimentally validated stack model, Eq.(2) is obtained.

$$\begin{aligned} P\left(T, ECSA\right) = 59410 + 36520\ T + 2906\ ECSA + \\ 2690\ T^2 + 654.6\ T \times ECSA - 424.3\ ECSA^2 \end{aligned} \tag{2}$$

In this map, the ECSA and stack temperatures are the inputs and the maximum stack gross power is the output. More information about the ECSA and its estimation are detailed in [22].

3.3.2. Maximum power ramp-up rate

To obtain the maximum ramp-up rate of power at each instant of time, the following calculation is used:

$$\frac{\Delta P}{\Delta t} = \frac{P_2 - P_1}{\Delta t} \tag{3}$$

where P_2 is the maximum power point regarding the stack's conditions of temperature and humidity that can be obtained using Eq.(2). P_1 is the measured power at each sampling time. Using (2) and the measurement stack's current and voltage, one has

$$P_2 = P\left(T, ECSA\right) \tag{4}$$

$$P_1 = V_1 I_1 = V_{stack} I_{stack} \tag{5}$$

The calculation of $\Delta(t)$ is given by,

$$\Delta t \approx \frac{I_2 - I_1}{\frac{dI(t)}{dt}} \tag{6}$$

Considering Eq.(2) and the technical characteristics of the stack, the minimum permissible output voltage of the stack at maximum power is $V_2 = 220$.

Therefore, the current at maximum power point can be calculated as follows:

$$I_2 = \frac{P_2}{V_2} = \frac{P\,(T, ECSA)}{220} \tag{7}$$

Based on the relationship between the stack current and the mass flow rate of inlet oxygen in Eq.(8), $\frac{dI(t)}{dt}$ can be calculated. Regarding the information that exists in the compressor's datasheet, maximum mass flow rate of the compressor is $max(\frac{d\dot{m}_{in}}{dt}) \approx 66(g/s^2)$. Therefore, Δt can be calculated and then, the maximum power ramp-up rate yields

$$\frac{dI(t)}{dt} = \frac{d\dot{m}_{O_{2in}}}{dt} \frac{4F}{M_{O_2} n_c} \frac{1}{\lambda_{O_2}} \tag{8}$$

3.3.3. Maximum instant power

Maximum instant power is the maximum net power that the system can deliver in the next sampling time (0,01s). Maximum instant power can be calculated based on the estimation of the maximum safe current that can be drawn from the stack in the next sampling time and the stack voltage in the next sampling time Eq.(10). The maximum safe current is equal to the DC-DC set-point current that will be explained in section 3.3.4. The stack's voltage in the next sampling time is equal to the measured stack voltage at the current time minus the increment of voltage drop due to activation loss, impedance losses, and concentration losses. So, the Maximum instant net power is calculated as follows.

$$P_{instantMax} = V_{nxtInst} \cdot (I_{dc-dc}) - P_{loss} \tag{9}$$

$$\begin{aligned} V_{nxtInst} = V_{measurment} - \Delta V_{Activation} - \\ \Delta V_{Impedance} - \Delta V_{Concentration} \end{aligned} \tag{10}$$

where $P_{instantMax}$ is the estimation of the maximum net power that the stack can deliver in the next sampling time $(k+1)T_s$; $V_{nxtInst}$ is the estimation of stack voltage in the next sampling time $(k+1)T_s$; The impedance loss $\Delta V_{Impedance}$ is calculated as follows

$$\Delta V_{Impedance} = R_{ohm}(I_{dc-dc} - I_{stack}) \tag{11}$$

where R_{ohm} is the Ohmic resistance of the stack obtained based on the simulation of the validated model;$\Delta V_{Activation}$ and $\Delta V_{Concentration}$ are neglected.

3.3.4. DC-DC set-point current

The fuel cell system supervisory controller estimates the safe current to be drawn from the stack. In automotive applications, fuel cells are exposed to challenging scenarios of rapid load changes[10]. Therefore, due to the compressor's dynamic behavior, air starvation is possible, and consequently, stack degradation can occur. To protect the stack from a load current shock that causes air starvation and increases the fuel cell degradation, using measurement of the inlet air to the stack at each sampling time, the maximum safe current that can be drawn from the stack is computed. Therefore, the fuel cell supervisory controller ensures that the drawn load current is the safe current that the stack can provide. This safe current which is the DC/DC converter setpoint is calculated as follows.

$$I(t) = \frac{\dot{m}_{total} 4F}{M_{dryair} n_c} \times \frac{0.2095}{(1 + HR)\lambda_{O_2}} \tag{12}$$

where $\dot{m}_{total}$ is the measured inlet mass flow rate and the HR is the ambient humidity ratio before the humidifier. The stoichiometry λ_{O2}, is set to the minimum permissible stoichiometry.

4. Automotive Run state test and experimental results

In this section, the purpose is to implement the proposed supervisory controller in an automotive proton-exchange membrane (PEM) fuel cell system (FCS). Several tests were performed to the integrated system in order to evaluate the performance, functionalities and durability of the FCS. After the FCS evaluation at PowerCell Sweden (PCS) facilities, the FCS was integrated into a vehicular platform to test the performance and drivability under automotive conditions. The automotive conditions tests were done in a vehicle rig at Chalmers University of Technology (CTH) and proving ground test at China Euro Vehicle Technology (CEVT) facilities as shown in Fig.6 This section will describe and evaluate the proposed fuel cell supervisory controller in the Run state. As discussed in the section on state-machine architecture, there are ten discrete states for the fuel cell system. It is assumed that the fuel cell system is already in the Run state at the beginning of this analysis. During the Run state, the optimum setpoint generator updates the subsystems' references based on the requested gross power from the vehicle side. In the Run state, the SM receives the subsystems setpoints from the optimal set-point generator and the DC/DC setpoint current from the power

(a) Vehicle rig at Chalmers University

(b) CEVT Proving Ground

Figure 6: Vehicle Test[23]

limit calculator and sends them to the different subsystems and the DC/DC converter. The block diagram of the FCSSC integrated with other auxiliary subsystems, anode subsystem, cathode subsystem, thermal subsystem, FC stack, vehicle control unit, propulsion parts, and diagnosis subsystem is shown in Fig.7 In the Run state, the following procedure is done in each iteration of the system operation, i.e., every 0.01 s.

- According to the driver acceleration decision, the signal of the net power requested by the traction motor is generated.
- According to the net power requested by the traction motor, the state of charge of the battery and the implemented energy management algorithm, the vehicle control unit sends the net power request to the fuel cell system.
- Using the compressor power consumption map, the compressor consumption is estimated and it is added to the requested net power to have the gross requested power.

$$P_{gross} = P_{net} + P_{compressor} \tag{13}$$

- The gross power requested is converted into current using the static polarization curve of the stack.

- The optimal setpoints corresponding to the load current for the three subsystems are generated inside the Optimal setpoint Generator block.
- The generated optimal setpoints of the three subsystems are sent to the subsystems' local controllers through the state machine.
- The Power Limit Calculator unit computes the available net power and power ramp-up capability using the stack temperature, stack hydration condition, voltage, current and estimation of other power loss of the system such as compressor and fans power consumption. The Power Limit Calculator unit directly sends this information as the stack net available power information to the vehicle control unit. Furthermore, the DC/DC converter setpoint current is calculated inside the Limit Power Calculator, and the state machine sends this information to the DC/DC converter as the DC/DC setpoint current.

4.1. Experimental results

In this section, the experimental results of the vehicle on the road for a standard driving cycle are presented. The test was done to evaluate the performance of the whole system in terms of produced power and load profile tracking and the performance of the balance of plant subsystem local controllers. Driving cycles address the change of speed in a specific period of time and its principal characteristics such as duration, average speed, maximum speed and the time related to idling, acceleration, deceleration, and consistent speed conditions. The Worldwide harmonized Light vehicles Test Cycles (WLTC) which are chassis dynamometer tests for the determination of emissions and fuel consumption from light-duty vehicles are used in this work. These driving cycles are commonly used in the automotive industry to evaluate the performance of the employed technology in the vehicle. Specifications of the used base vehicle are summarized in Table 3. The powertrain includes a High Voltage (HV) battery, with a total pack energy of 9.7 kWh at the beginning of life and peak power of 75 kW. The HV battery used in this prototype vehicle allows for different power split algorithms between the battery and FC. The split algorithm is implemented inside EMS.

4.2. Validation of stack model with experimental data

In this section, the logged stack current and the subsystem setpoints are used in Simulink to validate the stack and subsystems model and the subsystem local controller. Fig.8 shows the output net power of the stack in

Table 3: Base vehicle specifications

Engine	**Transmission**	**Curb weight (kgs)**		
Geely Engine Petrol 3 (GEP3)	Hybrid 7 Dual Clutch Transmission (7DCTH)	Front	Rear	Total
Max torque: 265 N, Max power: 132 kW	Max Torque: 164 Nm, Electrical power: 60 kW	1043	772	1815

the experimental data and simulated model. The magnified figure between $t = 550$ s to $t = 700$ s shows that the Simulink model output power, green line, follows the dynamic behavior of the real output power, blue liner, with good accuracy. The real output power is gross power and includes the compressor consumption as well. Therefore, there is a difference between the requested net power and the produced gross power.

4.3. Stack output power

The net power requested by the vehicle and the produced gross power of the stack are shown in Fig.9(a). The zoomed part between $t = 600$ s to $t = 800$ s shows that the fuel cell stack is able to provide the net power requested by the vehicle and follows the dynamic of the load. The difference between the produced gross power and the requested net power is the auxiliary power consumption (mainly due to the compressor) that the stack provides. As explained in the Run state procedure, the requested net power is converted to requested gross power first, then the setpoints are generated based on the requested gross power. Therefore, the produced gross power is more than the requested net power as expected. The Stack voltage and current are shown in Fig.9(b).

4.4. Subsystems local controllers' performance

In this section, the experimental results of the local controller's ability for setpoint achievement will be discussed. Considering the requirements of the project, three setpoints are defined for the cathode subsystem. Regarding the requested net power by the vehicle control unit, the three setpoints are inlet air mass flow rate, inlet air pressure and humidity ratio, which are generated by the optimal setpoint generator and sent to the cathode local controller. The pressure and inlet air humidity ratio setpoints were set to a constant value 1.13 bar and 0.04, respectively. Fig.10 indicates that the cathode subsystem local controller tracks the setpoints generated by the optimal setpoint generator very well. The thermal subsystem was designed and delivered by DLR. The main aspect for evaluation is how well the thermal subsystem is able to control the stack inlet coolant temperature and the outlet coolant

temperature or the differential temperature between the inlet coolant and the outlet coolant. The experimental results are shown in Fig11(a). It turns out that the thermal subsystem effectively controls the stack inlet coolant temperature and the stack outlet coolant temperature, although, the control parameters are dependent of each other. The anode subsystem was developed by the AVL and uses an injector-ejector to control the fuel pressure and increase the hydrogen utilization rate through recirculation. The anode subsystem controller controls the anode channel inlet hydrogen pressure and the purge rate in the anode loop. The pressure of the anode has to be controlled at a fixed quantity above the cathode inlet pressure based on the requirement of the project and stack safety. The anode inlet pressure and the hydrogen flow from tank are shown in Fig.11(b) .

4.5. Fuel cell system efficiency

To measure the efficiency of the system, the consumed hydrogen needs to be measured and the stack and fuel cell system efficiency can be calculated as (1). The subsystems' power consumption such as compressor and fan consumption is considered as the power loss to the fuel cell system. The fuel cell system efficiency considering the lower heating value of hydrogen ($120MJ/Kg$) and the lost power is shown in Fig.12, and it is around 56%. The lower heating value is considered because the state of the water exhaust of a PEM fuel cell stack is mostly vapor.

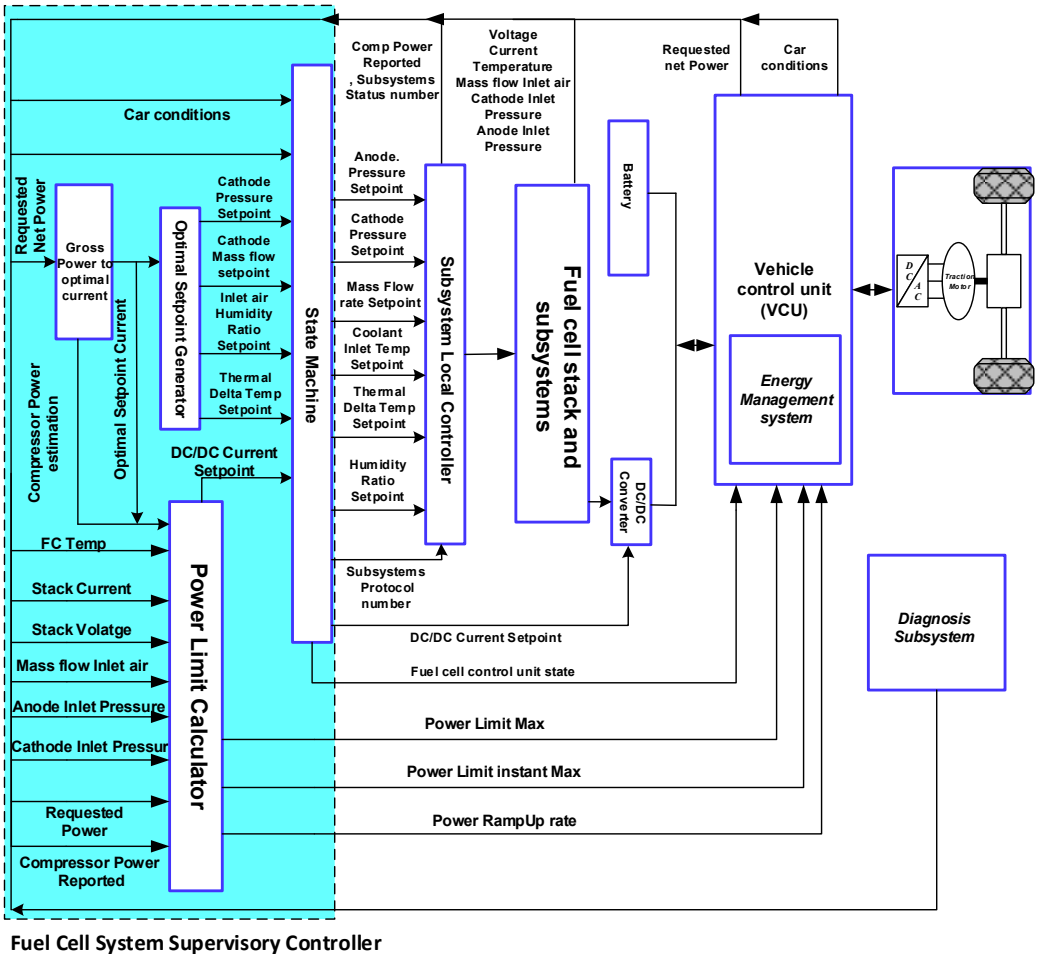

Figure 7: Block diagram of the proposed FCSSC integrated with the automotive fuel cell system

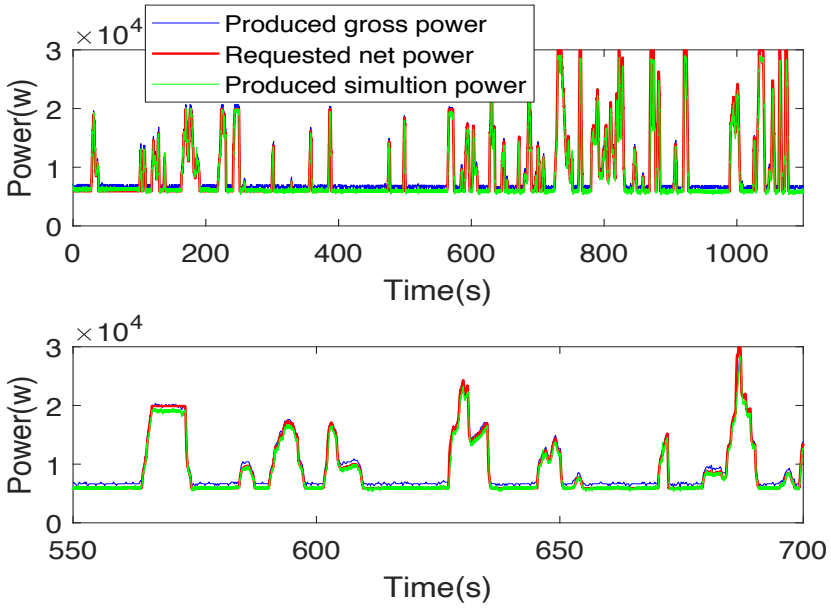

Figure 8: Output gross power of the real stack versus the output power of the Simulink model and the zoomed part between t = 550 s to t = 700s

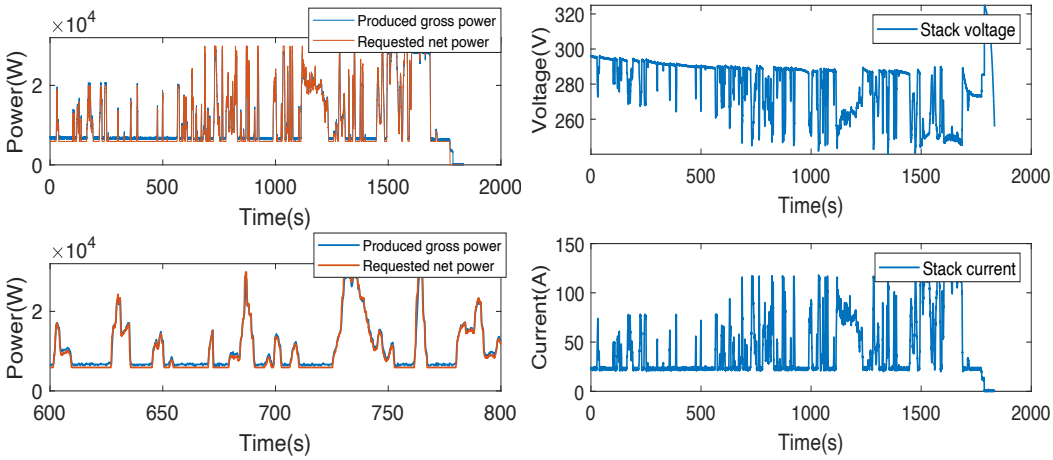

(a) Net power requested by the vehicle and the produced gross power and the zoomed part between $t = 600$ s to $t = 800$ s

(b) Stack voltage and current

Figure 9: Fuel cell Stack output measurements

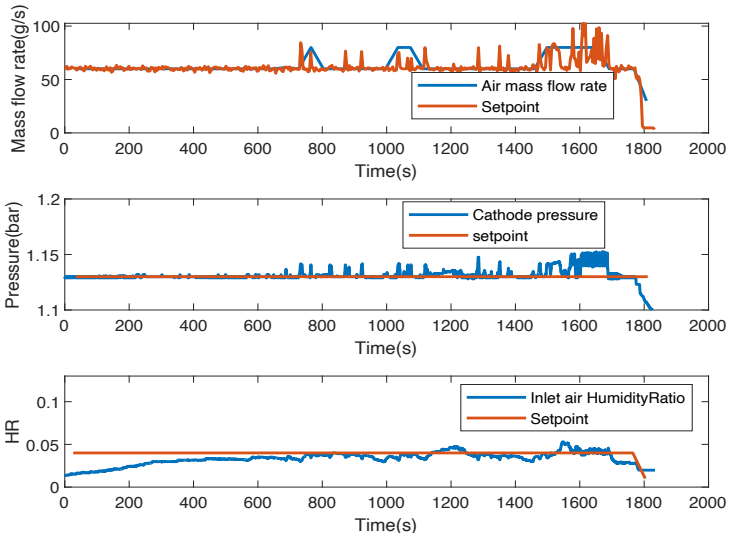

Figure 10: Performance of the cathode subsystem local controller to tracks the three setpoints of mass flow rate, pressure, and inlet air humidity ratio

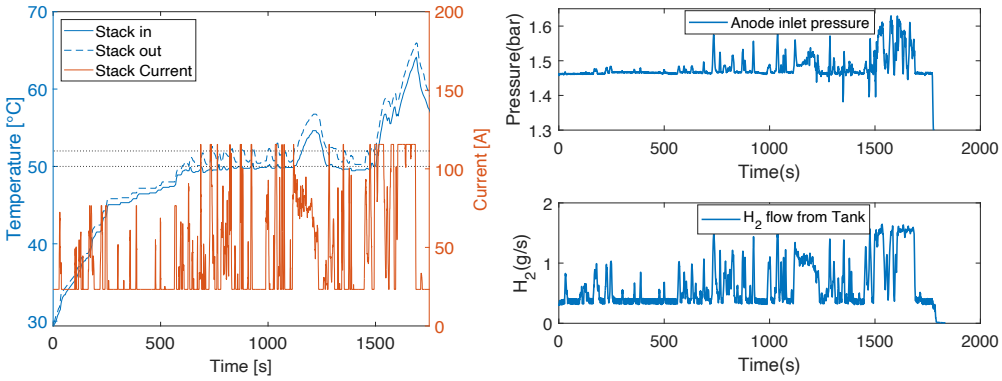

(a) Thermal subsystem setpoints and the setpoint achievement of thermal subsystem

(b) Anode inlet pressure and hydrogen flow from Tank

Figure 11: Anode and Thermal subsystem measurement parameters

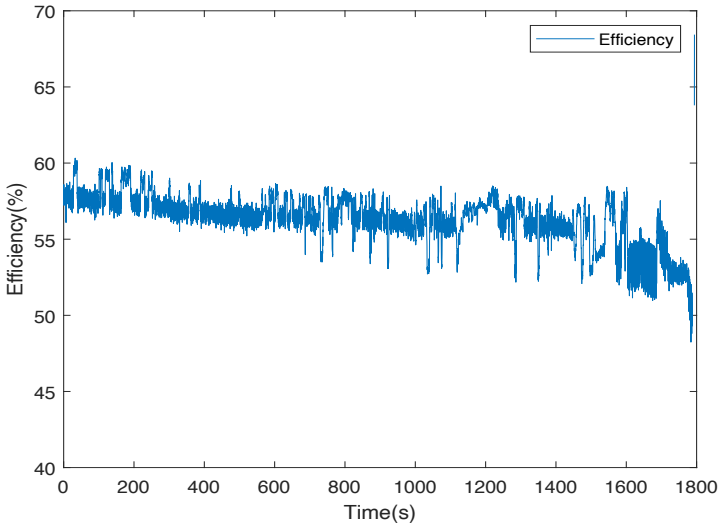

Figure 12: Fuel cell system efficiency

5. Conclusion

In this work, a PEM fuel cell system supervisory controller for an automotive application has been designed, implemented and validated through the INN-BALANCE developed prototype vehicle in PowerCell and CEVT facilities. The proposed fuel cell supervisory controller integrates three main parts: a state machine, an optimal setpoint generator and a power limit calculator. The Worldwide harmonized Light vehicles Test Cycles(WLTC) were used in this work to test the performance of the fuel cell systems in terms of load power dynamic tracking, subsystems local controller performance and ability to have a successful start-up and shutdown. Furthermore, the overall system performance and efficiency was studied. The key points of the work can be highlighted as follows:

- The proposed state machine as the heart of the supervisory controller gives the ability to the fuel cell system to have a successful startup and shutdown procedure, without any error or damage to the subsystem equipment due to turning on or off the subsystems incorrectly.
- During the test campaign of the prototype car, the proposed structure, specifically the state machine, gave this ability to the implementation team to easily find the operating state of the system and helped them to diagnose any errors during the test procedure. Therefore, the proposed structure is a simple and trustworthy method to design a fuel cell supervisory controller for vehicles and could be used in other applications.
- A previously experimentally validated stack model was used in the development process of the supervisory controller with high accuracy and reliability to test the controller which allowed for a successful implementation in the real car.
- The experimental results have shown that the subsystems local controllers were able to track the given setpoints properly. Furthermore, the fuel cell system was working properly as expected so that, the fuel cell system output power could follow the dynamic and the value of the power requested by the vehicle.

Acknowledgements

This work was supported in part by the Spanish national project DOVELAR (RTI2018-096001-B-C32, MINECO/FEDER) also in part by the Fuel Cells and Hydrogen 2 Joint Undertaking under Grant INN-BALANCE 735969.This Joint Undertaking receives support from the European Union's Horizon 2020 research and innovation program and Hydrogen Europe and N.ERGHY.

References

[1] C. Wang, M. Ricketts, A. P. Soleymani, J. Jankovic, J. Waldecker, J. Chen, and C. Xu, "Improved carbon corrosion and platinum dissolution durability in automotive fuel cell startup and shutdown operation," *Journal of The Electrochemical Society*, vol. 168, no. 3, p. 034503, 2021.

[2] J. Wang, H. Wang, and Y. Fan, "Techno-economic challenges of fuel cell commercialization," *Engineering*, vol. 4, no. 3, pp. 352–360, 2018.

[3] X. Guo, H. Zhang, J. Yuan, J. Wang, J. Zhao, F. Wang, H. Miao, and S. Hou, "Energetic and exergetic analyses of a combined system consisting of a high-temperature polymer electrolyte membrane fuel cell and a thermoelectric generator with thomson effect," *International Journal of Hydrogen Energy*, vol. 44, no. 31, pp. 16 918–16 932, 2019.

[4] H. Zhao and A. F. Burke, "Optimization of fuel cell system operating conditions for fuel cell vehicles," *Journal of Power Sources*, vol. 186, no. 2, pp. 408–416, 2009.

[5] T. Chu, M. Xie, Y. Yu, B. Wang, D. Yang, B. Li, P. Ming, and C. Zhang, "Experimental study of the influence of dynamic load cycle and operating parameters on the durability of pemfc," *Energy*, vol. 239, p. 122356, 2022.

[6] J. A. Salva, A. Iranzo, F. Rosa, E. Tapia, E. Lopez, and F. Isorna, "Optimization of a pem fuel cell operating conditions: Obtaining the maximum performance polarization curve," *International Journal of Hydrogen Energy*, vol. 41, no. 43, pp. 19 713–19 723, 2016.

[7] J. Han, S. Yu, and S. Yi, "Oxygen excess ratio control for proton exchange membrane fuel cell using model reference adaptive control," *International Journal of Hydrogen Energy*, vol. 44, no. 33, pp. 18 425–18 437, 2019.

[8] D. Hu, Y. Wang, J. Li, Q. Yang, and J. Wang, "Investigation of optimal operating temperature for the pemfc and its tracking control for energy saving in vehicle applications," *Energy Conversion and Management*, vol. 249, p. 114842, 2021.

[9] Y. Li, Z. Ma, M. Zheng, D. Li, Z. Lu, and B. Xu, "Performance analysis and optimization of a high-temperature pemfc vehicle based on particle swarm optimization algorithm," *Membranes*, vol. 11, no. 9, p. 691, 2021.

[10] T. Zhang, P. Wang, H. Chen, and P. Pei, "A review of automotive proton exchange membrane fuel cell degradation under start-stop operating condition," *Applied energy*, vol. 223, pp. 249–262, 2018.

[11] X. Yang, J. Sun, S. Sun, and Z. Shao, "An efficient cold start strategy for proton exchange membrane fuel cell stacks," *Journal of Power Sources*, vol. 542, p. 231492, 2022.

[12] A. Amamou, M. Kandidayeni, L. Boulon, and S. Kelouwani, "Real time adaptive efficient cold start strategy for proton exchange membrane fuel cells," *Applied Energy*, vol. 216, pp. 21–30, 2018.

[13] F. Jiang and C.-Y. Wang, "Potentiostatic start-up of pemfcs from subzero temperatures," *Journal of the Electrochemical Society*, vol. 155, no. 7, p. B743, 2008.

[14] F. Jiang, C.-Y. Wang, and K. S. Chen, "Current ramping: a strategy for rapid start-up of pemfcs from subfreezing environment," *Journal of The Electrochemical Society*, vol. 157, no. 3, p. B342, 2010.

[15] Q. Du, B. Jia, Y. Luo, J. Chen, Y. Zhou, and K. Jiao, "Maximum power cold start mode of proton exchange membrane fuel cell," *International journal of hydrogen energy*, vol. 39, no. 16, pp. 8390–8400, 2014.

[16] G. M. Ríos, J. Schirmer, C. Gentner, and J. Kallo, "Efficient thermal management strategies for cold starts of a proton exchange membrane fuel cell system," *Applied Energy*, vol. 279, p. 115813, 2020.

[17] H. Niu, C. Ji, S. Wang, M. Shi, H. Zhang, and C. Liang, "Analysis of the cold start behavior of a polymer electrolyte membrane fuel cell in constant power start-up mode," *International Journal of Energy Research*, vol. 45, no. 13, pp. 19 245–19 264, 2021.

[18] H. Chen, X. Zhao, T. Zhang, and P. Pei, "The reactant starvation of the proton exchange membrane fuel cells for vehicular applications: A review," *Energy conversion and management*, vol. 182, pp. 282–298, 2019.

[19] Z. Dong, X. Huang, Y. Dong, and Z. Zhang, "Multilayer perception based reinforcement learning supervisory control of energy systems with application to a nuclear steam supply system," *Applied Energy*, vol. 259, p. 114193, 2020.

[20] S. Di Cairano and I. V. Kolmanovsky, "Real-time optimization and model predictive control for aerospace and automotive applications," in *2018 annual American control conference (ACC)*. IEEE, 2018, pp. 2392–2409.

[21] J. C. Gómez, M. Serra, and A. Husar, "Controller design for polymer electrolyte membrane fuel cell systems for automotive applications," *international journal of hydrogen energy*, vol. 46, no. 45, pp. 23 263–23 278, 2021.

[22] J. Luna, E. Usai, A. Husar, and M. Serra, "Enhancing the efficiency and lifetime of a proton exchange membrane fuel cell using nonlinear model-predictive control with nonlinear observation," *IEEE transactions on industrial electronics*, vol. 64, no. 8, pp. 6649–6659, 2017.

[23] P. Haering, J. M. Garcia Campos, C. Mora González, M. Kogler, A. Molavi, J. Sanchez Monreal, E. Nordqvist, G. Oberholzer, D. Ramette, G. Montaner Rios *et al.*, *INN-BALANCE Guidebook. Improvement of Balance of Plant Components for PEM based automotive fuel cell systems*. Steinbeis-Edition, 2021.